

## Structural, Magnetic and Electrical Properties of Ba<sub>2</sub>Mg<sub>2</sub>Fe<sub>28</sub>O<sub>46</sub> (Mg<sub>2</sub>X) hexaferrites

Tahseen H. Mubarak, Olfat A. Mahmood, Zahraa J. Hamakhan\*

Department of Physics, College of Science, University of Diyala, Iraq.

\*Corresponding Author's email id: [za92ja@gmail.com](mailto:za92ja@gmail.com)

### Abstract

X-type barium hexaferrite having the formula Ba<sub>2</sub>Mg<sub>2</sub>Fe<sub>28</sub>O<sub>46</sub> (Mg<sub>2</sub>X) were prepared by sol-gel autocombustion method. The combusted powder calcined at different temperature for one hour. The effects of the annealing temperature on the structural, magnetic and electrical properties of the samples studied by X-ray diffraction (XRD), field emission scanning electron microscopy (FESEM), vibrating sample magnetometry (VSM) and LCR-meter. XRD results confirmed the formation of X-type barium hexaferrite with presence of secondary phases such as M and W phases at 1200°C and 1250°C but, single phase of X-type at 1300°C. Average crystallite size calculated by Scherer formula and showed it is equal 43.397 nm at 1300°C. FESEM images show platelet-like particles for X-type with average grain size about 1.154µm. Hysteresis loop measurements showed the values of the saturation magnetizations, remanence and coercivity at 1300°C about 50.656 emu/g, 18.416 emu/g and 505.330 Oe respectively. The dielectric constant, tangent loss and ac conductivity calculated as a function of frequency in the range of 100Hz to 3MHz for the samples sintered at 1200°C, 1250°C and 1300°C and showed that the dielectric parameters decrease with increasing frequency and increase with increasing temperature but the ac conductivity increases with increasing frequency and temperature and showed semiconducting like behavior with increasing temperature. Then concludes that high dielectric parameters and coercivity about 505.330 Oe at 1300°C made this material used in the fabrication of multilayer chip inductors (MLCI's) circuits.

**Keywords:** Hexaferrites; XRD; FESEM; Magnetic properties; Electrical properties.

### INTRODUCTION

Ferrites are technological very important compounds as they have versatile inherent nature. These materials are comprised of a mixture of iron oxide such as Fe<sub>2</sub>O<sub>3</sub> (hematite) or Fe<sub>3</sub>O<sub>4</sub> (magnetite) and the oxide of some other material other than iron [1]. Generally, ferrites are dark grey or black in visual aspect and are very hard and brittle ceramic materials having unique and useful properties [2]. They are cheap magnetic materials with excellent chemical stability. The multilayer chip inductors (MLCI's) and electromagnetic interface (EMI) materials have significant importance in high frequency applications [3]. Among various types of ferrites, the hexagonal ferrites are extensively studied materials as they have many practical applications and a vast era of production

for hard ferrites. As they exhibit the uniaxial anisotropy and strong coercive force, therefore these materials are also useful in permanent magnets [4,5]. Hexaferrites have gained great popularity after their discovery by Philips in 1950s [6]. Stable structural and magnetic properties, low cost manufacturing, cheap raw materials and electromagnetic absorption at hyper frequencies are the main reasons for the utilization of these materials instead of magnetic ferrites. In 1957, P. B. Braun was the first person who reported the crystal structure of Ba<sub>2</sub>Fe<sub>30</sub>O<sub>46</sub> (X-type) with real space coordinates for oxygen, barium and transition metal ions. In 1983 we reported for the first time the magnetic properties of Fe<sub>2</sub>X hexaferrite [7]. The anisotropy field (16 kOe) at room temperature is close to that of M and W-type hexaferrites. The chemical stability of the Fe<sub>2</sub>X compound is better than that of the Fe<sub>2</sub>W compound.

The X-type hexaferrites are ferrimagnetic materials which have many applications such as high-density perpendicular recording, magnetic refrigeration, magnetic recording media and microwave absorbers [8-10]. The magnetic properties may vary with the choice of the divalent cations and the way they are distributed among the sublattices. Therefore, it is interesting to study the effect of the substitution of Fe<sup>2+</sup> in the Fe<sub>2</sub>X hexaferrite with transition-metal ions on the magnetic properties. It is a difficult task to synthesis X-type ferrites owing to the mix up with M- and W-type ferrites phases [11]. The structure of X-type is constituted as a layer composed of R and S blocks stacked along the hexagonal c-axis likewise represented as: RSRSSR\*S\* R\*S\*S\*. The R block represents the BaFe<sub>6</sub>O<sub>11</sub> composition while S is for Fe<sub>6</sub>O<sub>8</sub> composition. R and S are three and two oxygen layers blocks respectively and asterisk indicates that the corresponding block is turned 180° along c-axis [12]. Usually very high temperature around 1250°C is required for synthesis of single phase X-type hexagonal ferrites. The goal of the present work to prepared the Ba<sub>2</sub>Mg<sub>2</sub>Fe<sub>28</sub>O<sub>46</sub> (Mg<sub>2</sub>X) hexagonal ferrites at different calcination temperature by using sol-gel autocombustion method and studying their structural, magnetic and electrical properties.

### EXPERIMENTAL WORK

#### Synthesis of Ba<sub>2</sub>Mg<sub>2</sub>Fe<sub>28</sub>O<sub>46</sub>

Sol-gel autocombustion method was used for synthesis of X-type barium hexaferrite with the formula Ba<sub>2</sub>Mg<sub>2</sub>Fe<sub>28</sub>O<sub>46</sub> using high-purity materials: (i) Barium nitrate Ba(NO<sub>3</sub>)<sub>2</sub> (General Purpose Reagent (GPR), 98 %), (ii) Iron nitrate nonahydrate Fe(NO<sub>3</sub>)<sub>3</sub>·9H<sub>2</sub>O (Central Drug House (CDH), 98

%),(iii)Citric Acid  $C_6H_8O_7 \cdot H_2O$  (Alpha Chemika, 99.5%),(iv) Magnesium nitrate hexahydrate  $Mg(NO_3)_3 \cdot 6H_2O$  (Himedia, 99 %).

The mixture of metals nitrates with Ba:Mg:Fe stoichiometric ratio is 2:2:28 and citric acid were dissolved in 300 ml of distilled water with 1:1 M ratios to form aqueous solutions with continuous magnetic stirring at room temperature for 30 min on a hot-plate magnetic stirrer. Citric acid was used as a fuel because of having better complexing ability, low ignition temperature (200-250°C), and controlled combustion reaction with nitrates. In addition, the metal ions distributed homogenously with the helped of chelating agent [13]. When the solution blended and complete dissolution for the raw materials, then liquid ammonia was slowly added to neutralize solution until PH=7 with continuous stirring. The temperature of hot plat-stirrer being increased gradually to reach (80°C) with continuous stirring and kept heating at this temperature for half an hour to stabilize the sol, then increase to (100°C),the water was evaporated from the solution and the sol gradually changes into gel, the solution color at this stage was recorded golden yellow. Then formed viscous gel, as the temperature increased to 200°C,the viscous gel started to bubbles and then combust due to the presence of citric acid. During the combustion process, the gel expanded rapidly and made a loose and fluffy powder [14]. Then, the powder put in oven for drying at (110°C) for half an hour. The powders were then calcined at 900 up to 1300°C for 1 h in air to create X-type hexaferrite. These powders were cooled down in the furnace so that the cations fitted at their equilibrium positions. After that ,we removed amount of powders for measuring the structural and magnetic properties. Then weighed 3gm of the powders which calcined at 1200°C, 1250°C and 1300°C to pressing within the cylinder mold under the pressure 4500 pounds per 1.6 inch to form the disks shape, then sintered later in the same temperature (1200°C, 1250°C and 1300°C) for 1 h. After that the thickness of the disks adjusted to 2.9 mm to using in electrical test.

### Characterization techniques

The structure of X-type barium hexaferrite was studied by X-ray diffraction method used to investigate the crystalline phase, crystallite size and lattice parameters [15]. 6000 X-Ray Diffractometer, with Cu-K $\alpha$  radiation source of wavelength  $\lambda = 1.54 \text{ \AA}$ . XRD diffraction patterns for the samples were recorded over the angular range  $20^\circ < 2\theta < 80^\circ$  with scan speed  $8.0000^\circ/\text{min}$ . The morphology of the particles in the prepared samples was examined using the Field Emission Scanning Electron Microscope (FESEM- MIRA3 model). The magnetic measurements were carried out at room temperature in an applied field up to 15 kOe using a vibrating sample magnetometer (VSM-LBKFB model). The dielectric parameters and ac conductivity ( $\sigma_{ac}$ ) measured at room temperature using LCR-meter-8105G model as a function of frequencies in the range of 100 Hz to 3MHz.

## RESULTS AND DISCUSSIONS

### XRD results

Fig. 1 indicates the X-ray diffraction (XRD) patterns of the powders with  $Mg_2X$  stoichiometry calcined at different temperatures (900°C,1100°C, 1200°C,1250°C and 1300°C) for one hour. At 900°C, comprises M-type ( $BaFe_{12}O_{19}$ ) ferrites and  $Ba_3Fe_{32}O_{51}$ (ICDD Card no.00-041-0846), increasing the temperature to 1100°C, the sample contained a mixture of M-type ( $BaFe_{12}O_{19}$ ) (ICDD Card no.00-027-1029) ferrites and W-type ( $BaMg_2Fe_{16}O_{27}$ ) with (ICSD Card no.01-078-1551). At 1200°C,X-type hexagonal ferrite formed with presence of W-type and  $Ba_3Fe_{32}O_{51}$ . After annealed at 1250°C, X-type became the major phase with one position corresponding to W-type and  $Ba_3Fe_{32}O_{51}$  phases.

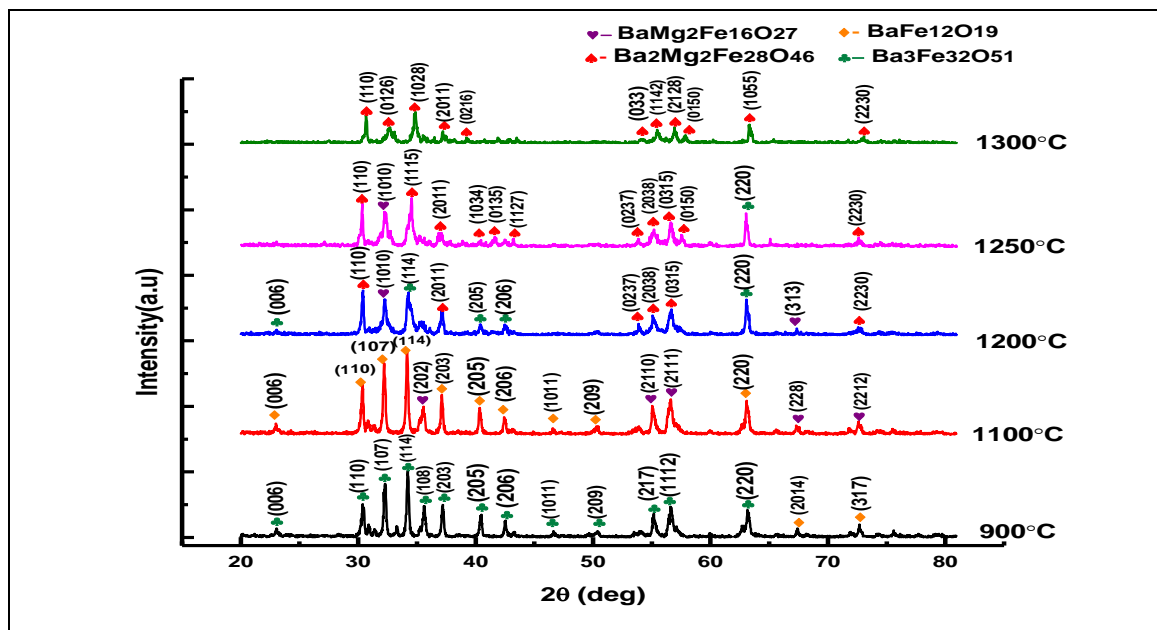


**Figure 1.** XRD patterns of the powders calcined at different annealing temperatures for formation (X-Type).

The presence of secondary phases in this samples is an indication that the calcination temperature was not high enough to induce complete for the production of pure Mg<sub>2</sub>X hexaferrite phase. With increasing the temperature to 1300°C, the peaks shifting to lower angles due to the phase transition to single phase Mg<sub>2</sub>X barium hexaferrite with group space (p63/mmc) and matched with standard pattern (ICSD Card no.01-073-2034) [16]. The intensity of the peaks differs from those described in the reference standard and this is due to the preferred orientation of the hexagonal plates found in the material structure [17].

Table 1 shows the results of the lattice constants 'a' and 'c', c/a ratio, cell volume, X-ray density, bulk density, porosity and crystallite size for X-type barium hexaferrite. The lattice parameters (a and c) were calculated from the XRD data using the following equation [18]:

$$\frac{1}{d^2} = \left[ \frac{4}{3a^2} (h^2 + hk + k^2) + \frac{l^2}{c^2} \right] \quad (1)$$

Where 'hkl' are the corresponding indices of each line in the pattern. The values of the lattice parameters 'a' and 'c' are in close agreement with the reported values for hexagonal ferrites [19]. The lattice parameters variation for different causes: Variation of stresses within the phases, temperature variation, changes in the chemical composition of the phases. The variation of 'a' is slightly but, 'c' sharply variation, 'c' decreases with increasing temperature from 1200°C to 1250°C due to the redistribution of cations between tetrahedral and octahedral sites, or due to the produced large number of vacancies at elevated temperatures and could be related with lattice distortions, then increases at 1300°C due to the grain growth, c/a ratios showed that these prepared material belong to hexaferrites family and thus X-type hexagonal structure has been confirmed from XRD data [20].

Cell volume calculated from the following equation [21]:

$$V = \frac{\sqrt{3}}{2} a^2 c \quad (2)$$

The values of the cell volume in close agreement with the reported values for hexagonal ferrites [19]. Unit cell volume decreases with increasing temperature from 1200°C to 1250°C which is related to the decrease in lattice constant 'a' and 'c', then increases at 1300°C due to the removal of lattice defects at higher sintering temperature and lattice relaxation.

The X-ray density (D<sub>x</sub>) calculated from the following equation [21]:

$$D_x = \frac{3M}{N_A V} \quad (3)$$

Where M is the molecular mass of Mg<sub>2</sub>X, N<sub>A</sub> is the Avogadro number and V is the volume of the unit cell. This variation in X-ray density for X-type barium hexaferrite with different annealing temperature were due to the variation in unit cell volume as X-ray density is inversely proportional to the cell volume which increases with increasing cell volume and

decreases with decreasing it [22] and also due to the presence of phase impurity in lattice.

The bulk density (D<sub>b</sub>) calculated from the following equation [21]:

$$D_b = \frac{m}{\pi r^2 h} \quad (4)$$

Where  $V = \pi r^2 h$ , and 'r', 'm' and 'h' are the radius, mass and thick- ness of the pellet respectively.

The porosity calculated from the following equation [21]:

$$P = \left( 1 - \frac{D_b}{D_x} \right) \quad (5)$$

Bulk density (D<sub>b</sub>) and porosity (P) are consider very important parameters for describing the physical properties of materials. The relation between bulk density and porosity as a function of temperature shown in fig. 2. The porosity increases with increasing temperature from 1200°C to 1250°C, then decreases at 1300°C, The porosity increases when small vacancies collection together to form the large vacancy with increasing temperature and decreases in porosity was due to the decrease in x-ray density and presence of compressive stress in the lattice which produces from the negative micro strain [23].

The decrease in density at 1250°C which may be due to existence of pores produced through sintering process at this temperature [24].

Bulk density was observed to be lesser than the x-ray density value and cannot exceed it, due to the sample contains cracks and pores on the macroscopic scale and vacancies in the lattice on the atomic scale [21].

Average crystallite size determined from the position of the strongest three peaks using Scherer's formula [21] as shown in equation (6) and fig.3. shows the relation between average crystallite size with temperature for X-type barium hexaferrite.

$$S = K \lambda / \beta \cos \theta \quad (6)$$

Where 'K' is a constant (0.89 for hexaferrite), 'λ' is the wavelength 1.5406 Å, 'β' is the line broadening at the middle of the maximum intensity (FWHM). Average crystallite size for X-type in the range (29.145-43.397) nm, decreasing in average crystallite size from 1200°C to 1250°C accordance with the previous study [25] due to the defects, secondary phase in the lattice inhibits the grain growth [26] and phase transition from other types of barium hexaferrite to X-type and also due to the peaks shifting to the higher angles, then increases at 1300°C due to the formation single phase of X-type barium hexaferrite when shifting to lower angles and removing the secondary phases.

**Table 1:** Lattice constants a and b, c/a ratio, Unit cell volume, x-ray density, Bulk density, Porosity and average crystallite size for Mg<sub>2</sub>X barium hexaferrite at different calcination temperature.

Parameters	1200°C	1250°C	1300°C
Lattice constant a (Å)	5.875	5.885	5.819
Lattice constant c (Å)	84.125	83.026	85.393
c/a ratio	14.319	14.108	14.674
Unit cell volume (Å) <sup>3</sup>	2515.443	2491.015	2504.919
X-ray density (gm/cm <sup>3</sup> )	5.194	5.245	5.216
Bulk density (gm/cm <sup>3</sup> )	3.118	2.712	3.162
Porosity	0.399	0.482	0.393
Average crystallite size (nm)	35.804	29.145	43.397

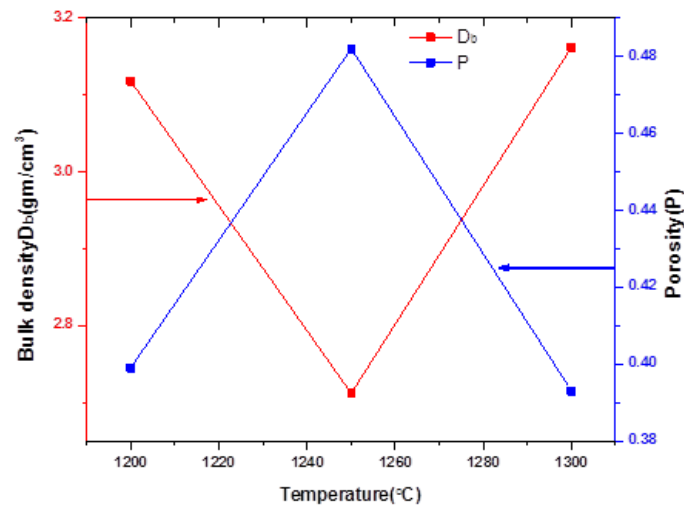


**Figure 2.** Behavior of bulk density and porosity with increasing temperature.

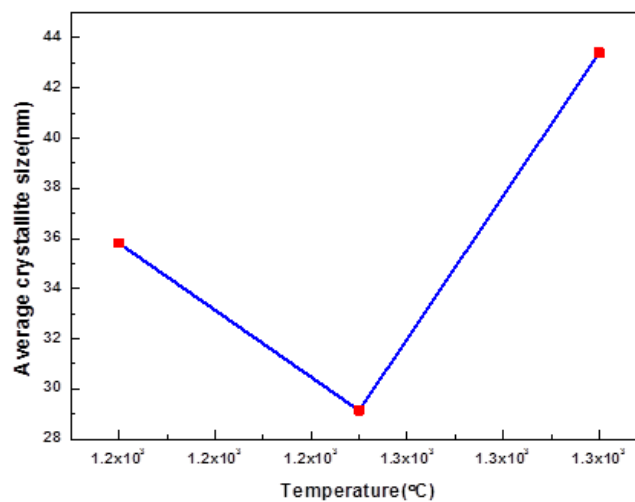


**Figure 3.** Behavior of average crystallite size with increasing temperature.

### FESEM results

Fig.4. shows the FESEM images for the sample calcined at 1200°C for 1h at low and high resolution (25.0 and 100) kx on a scale of 500 nm and 2 µm. Accordance with XRD results, the images show the presence of a combination of platelet-like, irregular particles and rod-shaped due to the existence of

different phases such as (M and W-type). X-type with hexagonal platelets like-layer formation and homogeneously arrangement with average grain size about (1.154µm) calculated using (Image-J software, version 1.47). It has been reported that hexagonal with platelets like used in microwave absorbing material [27].

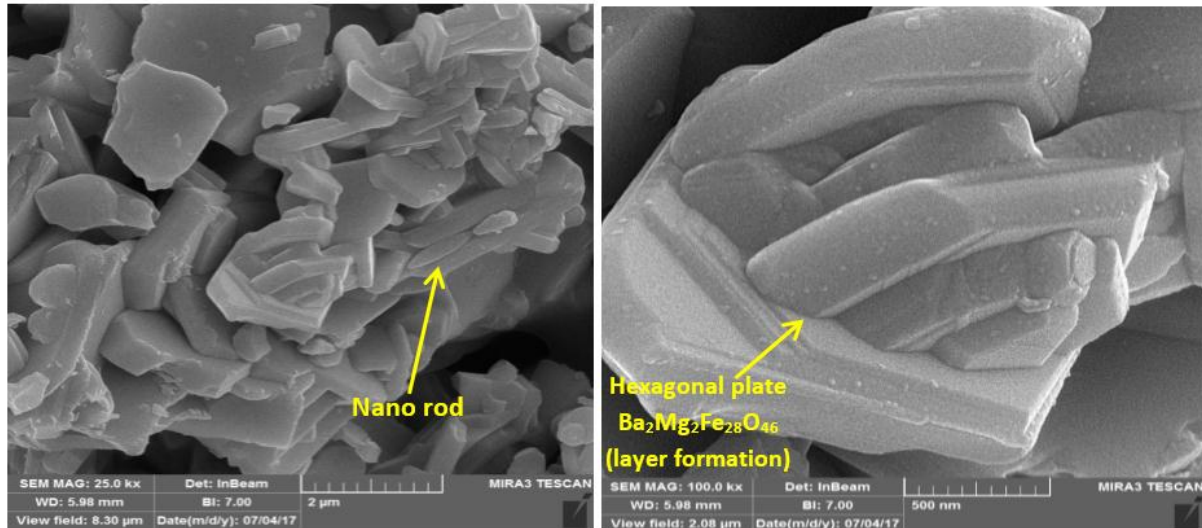


**Figure 4.** FESEM images for Mg<sub>2</sub>X barium hexaferrite at 1200°C for 1h.

### Magnetic results

Fig.5. shows the hysteresis loops for the X-type barium hexaferrite at different calcination temperature (1200°C, 1250°C and 1300°C) were measured using vibrating sample Magnetometer at room temperature. The shape and the width of the hysteresis loop depend on factors such as chemical composition, cation distribution and grain size. Width of loops showed hard characteristic for the sample calcined at 1200°C, but soft characteristic at 1250°C and 1300°C. These results are in agreement with the XRD results which showed the presence of nanocrystalline BaM phase (hard magnetic material) at 1200°C and decreases the crystallinity of BaM phase with increasing the temperature to 1250°C, then removed each secondary phases at 1300°C and formed X-type with soft magnetic character. Various magnetic properties such as saturation magnetization (M<sub>s</sub>), remanence (M<sub>r</sub>), coercivity (H<sub>c</sub>) and squareness ratio (M<sub>r</sub>/M<sub>s</sub>) for X-type barium hexaferrite shown in Table 2. The saturation magnetization increased with increasing temperature up to 1250°C from 51.250 emu/g to 59.448 emu/g, this behavior is attributed to the contribution of the BaM phase. The reported value for pure BaM phase is 72 emu/g [1] which is higher than the pure X-type barium hexaferrite [19], then decreased at 1300°C to 50.656 emu/g for removing secondary phase and formation soft magnetic material (X-type). The remanence magnetization decreased with increasing temperature due to the transition from hard to soft magnetic material. Also, the coercivity decreased with increasing temperature which is related to the transformation from the hard BaM magnetic phase to the softer W- and X-type phases and grain size growth. The

relation between saturation magnetization, remanence and coercivity as a function of increasing temperature shown in Fig.6. The squareness ratio M<sub>r</sub>/M<sub>s</sub> for the X-type is also given in Table 2. It has been reported that if the squareness ratio is greater than 0.5 (M<sub>r</sub>/M<sub>s</sub> ≥ 0.5), then the compounds are in single magnetic domain and if this ratio is less than 0.5 (M<sub>r</sub>/M<sub>s</sub> ≤ 0.5), then the compounds are in multi-magnetic domains. It has been observed for all samples that the squareness ratio less than 0.5, that confirmed the multi-magnetic domain structure [28]. It is well known that particle size has a significant effect on the magnetic properties of the magnetic materials. When the particles are smaller than the critical single domain size they are mainly in single domain (the critical single domain size of less than 1 µm for hexaferrites) [29]. When the particle size becomes bigger than the critical value, most of them would exist in multi-domain. With an increase in the sintering temperature the particle size also increases towards the critical single domain size. As a result, the saturation magnetization (M<sub>s</sub>), remanence (M<sub>r</sub>) and coercivity (H<sub>c</sub>) increases eventually reaching a maximum value at single domain size because of the coherent rotation of spins. The value of magnetization, remanence and coercivity begin to decrease when the particles become larger than the single domain size at higher temperature as a result of their coalescence with each other.

This phenomenon could also be ascribed to the transition from magnetic single domain to magnetic multi-domain structure through the increase in particle size with the increase in synthesis temperature [30].

**Table 2:** Saturation magnetization( $M_s$ ), remanence( $M_r$ ), coercivity and squareness ratio( $M_r/M_s$ ) with increasing temperature.

$T(^{\circ}\text{C})$	$M_s(\text{emu/g})$	$M_r(\text{emu/g})$	$H_c(\text{Oe})$	$M_r/M_s$
1200	51.250	26.051	1329.409	0.508
1250	59.448	22.173	650	0.372
1300	50.656	18.416	505.330	0.363

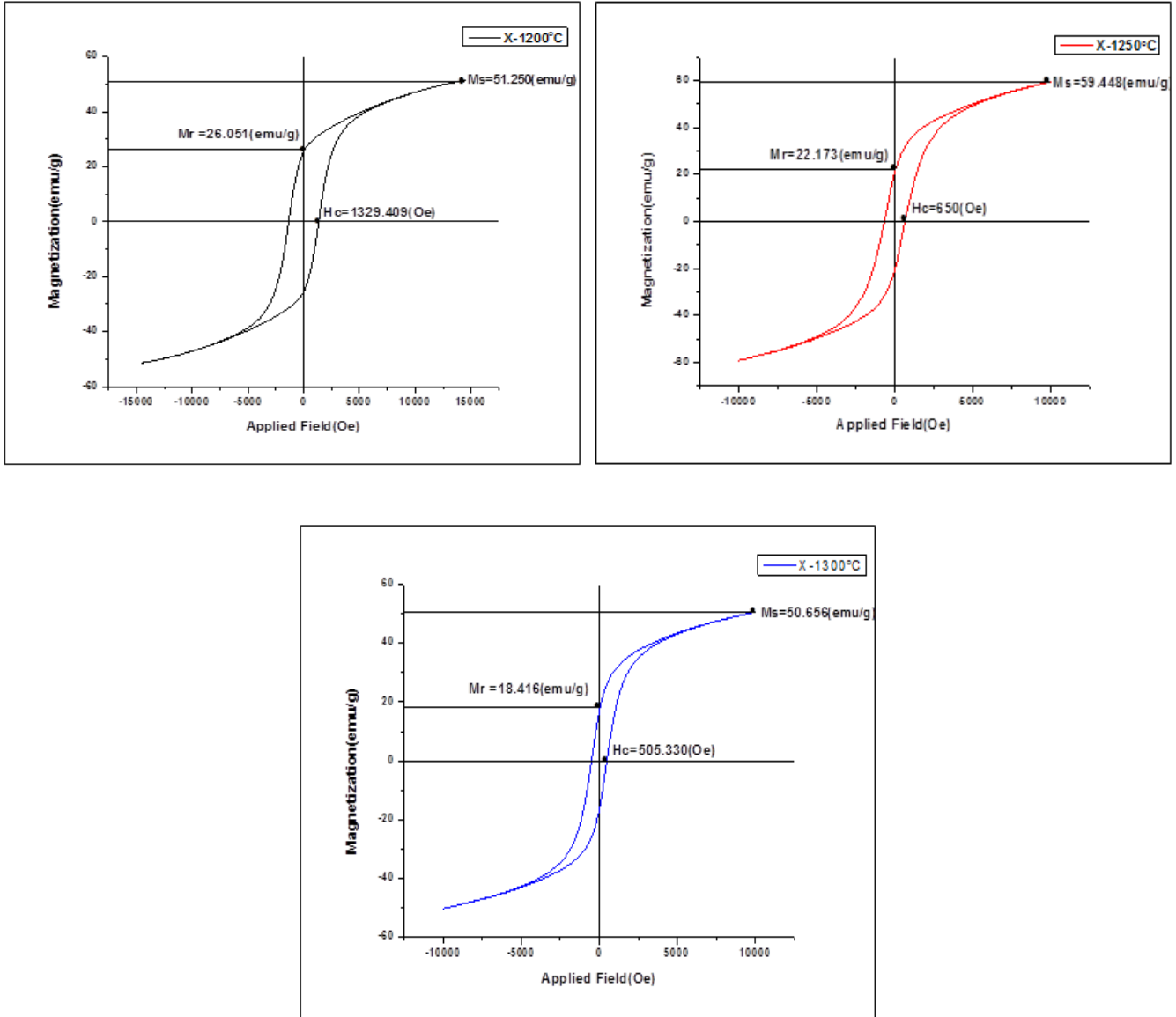


**Figure 4.** Hysteresis loops for  $\text{Mg}_2\text{X}$  barium hexaferrite calcined at  $1200^{\circ}\text{C}$ ,  $1250^{\circ}\text{C}$  and  $1300^{\circ}\text{C}$ .

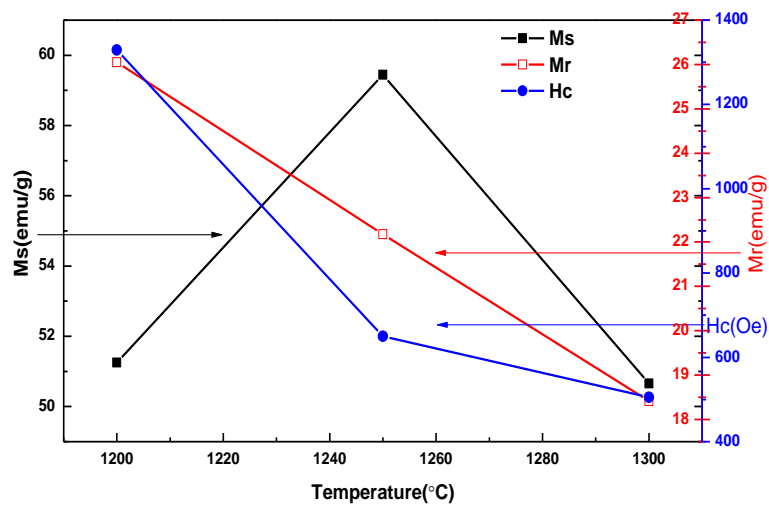


**Figure 6.** Behavior of saturation magnetization, remanence and coercivity with increasing temperature.

### Electrical results

The electrical properties such as dielectric constant, tangent loss, and electrical conductivity studied for X-type barium hexaferrite which sintered at (1200°C, 1250°C and 1300°C) and shown in fig.7,8,9 respectively. Dielectric constant is one of the important electrical properties of dielectric materials. It depends strongly on the frequency of the alternating electric field, chemical structure, defects of the material, the method of preparation, cations in interstitial sites of unit cell of ferrite samples, porosity and grain size. The dielectric constant ( $\epsilon'$ ) as a function of frequency for the samples was studied. It was observed that all the samples have higher dielectric constant at low frequency and then decreased gradually with increasing frequency, this behavior is typical of ferrites and a similar behavior was observed by other researchers [31,32]. The variation in the dielectric constant can be explained on the basis of arising polarization in response to the frequency and electron exchange phenomenon in the ferrites material.

At lower frequencies, the dielectric constant is high due to the electron exchange between the  $\text{Fe}^{3+}$  and  $\text{Fe}^{2+}$  in the direction of the applied field takes place on the octahedral sites of the material which produce the polarization in the material [23]. The tendency can be explained on the basis presence of four different types of Polarization at lower frequencies (i.e. Electronic, ionic, dipolar and space charge) contributions take a part in the dielectric constant, but the decrease in dielectric constant at higher frequency with increasing frequency related to the applied field at higher frequency becomes larger than the electron exchange (hopping) frequency therefore, charge carriers require a finite time to line up their axes in the direction of an applied alternating field as a result the electron exchanges process lags behind and produce its own field in reverse direction of the applied field which oppose the electron exchange phenomenon. This reduces the possibility of electrons reaching the grain boundary and as a result polarization decreases and relax out

resulting thereby in the decrease of dielectric constant with an increase in frequency [32,23]. This variation in the dielectric constant with the frequency can also be explained on the basis of space charge polarization. This can be explained on the basis of Maxwell-Wagner model [32]. According to this model, the dielectric structure was supposed to be composed of well conducting grains separated by the poorly conducting grain boundaries. The electrons reach the grain boundary through hopping and if the resistance of grain boundary is high enough then electrons pile up there and produce polarization. Therefore the grain boundaries considered as a major role and effective at lower frequencies and the conducting ferrites grains play important role at higher frequencies. Many researchers reported similar type of behavior of dielectric constant with frequency in the case of hexagonal ferrites [23].

The value of dielectric constant becomes constant due to the electron exchange between  $\text{Fe}^{2+}$  and  $\text{Fe}^{3+}$  ions does not follow the variations in applied field as the frequency increased beyond a certain limit. Sintering at higher temperature enhances the  $\text{Fe}^{2+}$  ions, which are more conducting ions as compared to other cations present in ferrites. The sample which sintering at 1300°C have higher dielectric constant decreases exponentially with increasing in frequency, this behavior is due to the enlarge grain size and presence of more  $\text{Fe}^{2+}$  ions showed high polarizing while decreasing at 1200°C and 1250°C.

Fig. 8 shows the variation of tangent loss as a function of frequency. The values of tangent loss depends on the different elements such as, structural homogeneity,  $\text{Fe}^{2+}$  contents, and sintering temperature [33]. Tangent loss for all the samples decreases with increasing in frequency and increases with increasing temperature. The abnormal dielectric behavior for all the samples can be explained on the basis of Rezlescu model which states that the relaxation peaks may be formed when the charge carriers of both p and n type collective

contribution [23]. Also the abnormal dielectric behavior can be ascribed to the conduction mechanism through the positive holes and electrons which arises due to the loss of oxygen during sintering and/ or substitution of metal ions. The conduction mechanism is mainly due to the hopping of electrons between  $Fe^{3+}$  and  $Fe^{2+}$  at octahedral sites. Resonance occurs when the hopping frequency becomes nearly equal to the externally applied frequency, which leads to the creation of the relaxation peak [34].

Fig.9 shows the variation of the A.C conductivity as a function of frequency. The A.C conductivity increases with increasing in frequency and this behavior can be explained on the basis the applied field which eases in transporting the charge carriers between different localized states in addition

to liberate the trapped charges from different trapping centers. At lower frequencies, the hopping electron between  $Fe^{3+}$  and  $Fe^{2+}$  is less due to the grain boundaries are very active at lower frequency, but the hopping of electron is high at higher frequency due to the conductive grains become much active in upholding the hopping of electron between  $Fe^{3+}$  and  $Fe^{2+}$  ions. The sample was sintered at  $1300^{\circ}C$  has high conductance for presence of more  $Fe^{2+}$  ions and decreases in porosity. In case of ferrites, the conduction current constitute when the electron hopping from  $Fe^{2+}$  to  $Fe^{3+}$  or vice-versa which leads to the creation of extra electron or hole. Under the influence of external electrical energy or thermal energy, these extra electrons (or holes) jump from one valence state of iron to the other and create the conduction current [32].

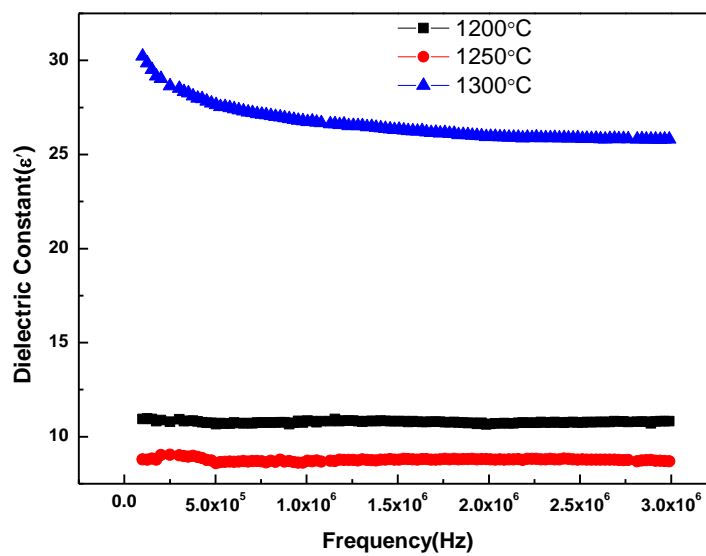


Figure 7. Dielectric constant( $\epsilon'$ ) for  $Mg_2X$  barium hexaferrite at different sintering temperature as afunction of frequency(Hz).

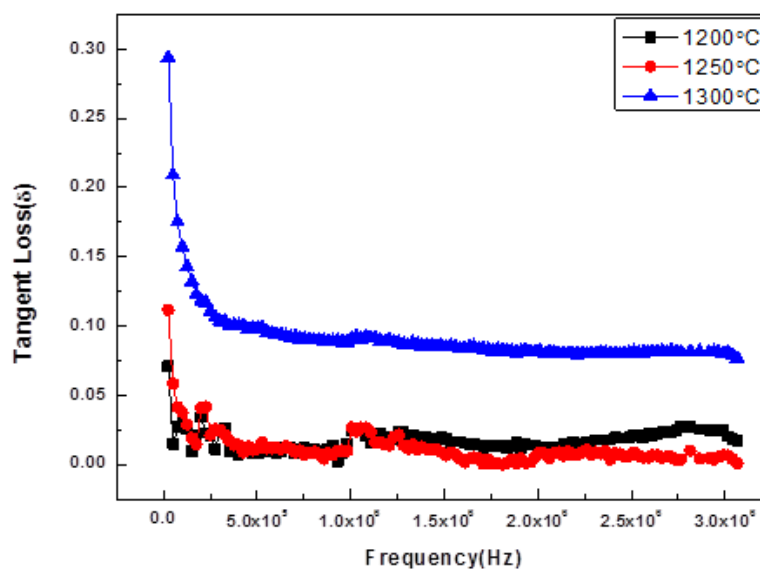
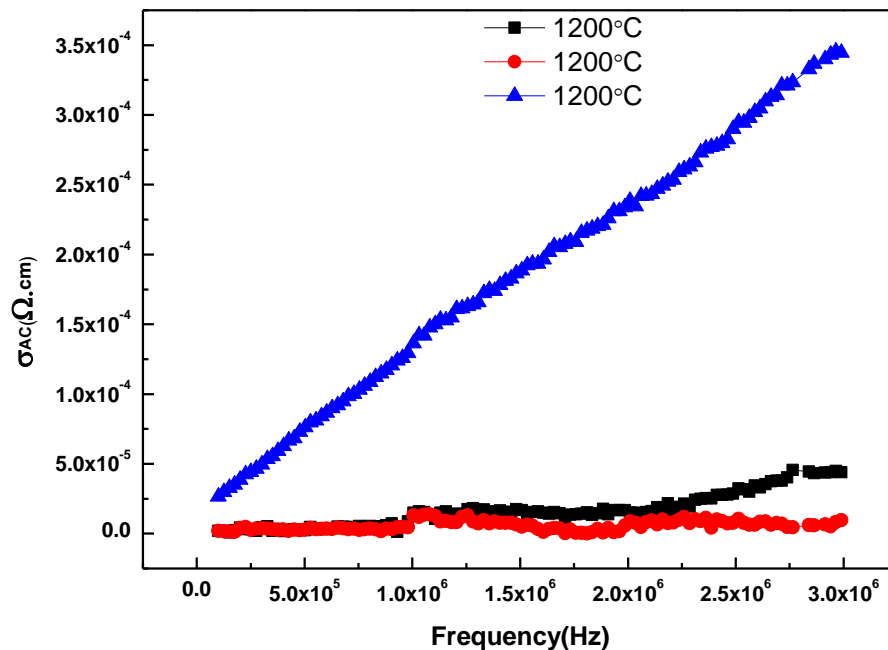


Figure 8. Tangent loss( $\delta$ ) for  $Mg_2X$  barium hexaferrite at different sintering temperature as afunction of frequency(Hz).



**Figure 9.** A.C conductivity( $\sigma_{AC}$ ) for  $Mg_2X$  barium hexaferrite at different sintering temperature as a function of frequency(Hz)

## CONCLUSIONS

- 1) Sol gel auto combustion is a suitable method for preparation single phase of X-type barium hexaferrite with homogeneous and ultrafine ferrite powders.
- 2) X-type barium hexaferrite with single phase formed at 1300°C. At 1200°C and 1250°C, X-type formed as a major phase with little position corresponding to  $Ba_3Fe_{32}O_{51}$  and  $BaMg_2Fe_{16}O_{27}$ . At 900°C and 1100°C show secondary phases ( $BaFe_{12}O_{19}$  and  $Ba_3Fe_{32}O_{51}$ ), ( $BaFe_{12}O_{19}$  and  $BaMg_2Fe_{16}O_{27}$ ) respectively. Then concludes that 1300°C is a suitable temperatures for preparing single phase X-type with high intensity.
- 3) X-type barium hexaferrite with platelet-like grains were detected from FESEM images is suitable for the purposes of microwave absorbing.
- 4) VSM measurements show that the coercivity and magnetization values are strongly dependent on the calcination temperature and particle size, the coercivity and remanence decrease with increasing temperature but, the saturation magnetization increases with increasing temperature after that decreases at 1300°C when formed single phase X-type barium hexaferrite.
- 5) Magnetization against applied field curve shows soft magnetic character for X-type barium hexaferrite when the coercivity decreases with increasing temperature.
- 6) The squareness ratio( $M_r/M_s$ ) decreases with increasing temperature and showed it is less than 0.5 confirmed that the compound is in multi-magnetic domains structure.
- 7) LCR-meter tests show higher dielectric constant and tangent loss ( $\tan\delta$ ) at low frequency and then decreased

gradually with increasing frequency but increase with increasing temperature.

- 8) The A.C conductivity gradually increases with an increasing in frequency and temperature.
- 9) X-type barium hexaferrite has semiconducting like behavior, where the ac conductivity increases with increasing temperature
- 10) X-type barium hexaferrite at 1300°C has high dielectric parameters and coercivity about 505.330 Oe suggested that this hexagonal ferrite can be used in the fabrication of multilayer chip inductors (MLCI's) circuits.

## REFERENCES

- [1] J. Smith, H. Wijn, Ferrites, Eindhoven: Philips' Technical Library, (1959).
- [2] M. Sugimoto, The past, present, and future of ferrites, Journal of the American Ceramic Society, 82 (1999) 269-280.
- [3] I. Ali, N. Shaheen, M. Islam, M. Irfan, M.N. Ashiq, M.A. Iqbal, A. Iftikhar, Study of electrical and dielectric behavior of  $Tb^{+3}$  substituted Y-type hexagonal ferrite, Journal of Alloys and Compounds, 617(2014) 863-868.
- [4] S. Farooq, Study of electrical and magnetic properties of strontium-barium hexaferrite nanomaterials for potential technological applications, Quaid-i-Azam University Islamabad, 2010.

- [5] I. Ali, M. Islam, M.N. Ashiq, H.M. Khan, M.A. Iqbal, M. Najam-Ul-Haq, Effect of Eu–Ni substitution on electrical and dielectric properties of Co–Sr–Y-type hexagonal ferrite, *Materials research bulletin*, 49 (2014) 338-344.
- [6] Y. A. Farzin, O. Mirzaee, A. Ghasemi, Synthesis behavior and magnetic properties of Mg-Ni co-doped Y-type hexaferrite prepared by sol-gel auto-combustion method, *Journal of Material Chemistry and Physics*, xxx (2016) 1-11.
- [7] B. X. Gu, Magnetic properties of Xtype  $Ba_2Me_2Fe_{28}O_{46}$  (Me=Fe, Co, and Mn) hexagonal ferrites, *Journal of applied physics*, 71 (1992)5103.
- [8] E. M. Chudnovsky, L. Gunther, Quantum Tunneling of Magnetization in Small Ferromagnetic Particles, *Journal of physical review letters*, 60 (1988) 661-755.
- [9] A. Aharoni, Introduction to the Theory of Ferromagnetism, Oxford University Press, New York, 1996.
- [10] R.D. McMichael, R.D. Shull, L.J. Swartzendruber, L.H. Bennett, Magnetocaloric effect in superparamagnets, *Journal of Magnetism and Magnetic Materials*, 111(1992) 29-33.
- [11] K. Kamishima, T. Mashiko, K. Kakizaki, M. Sakai, K. Watanabe, H. Abe, Synthesis and magnetic characterization of Sr-based  $Ni_2X$ -type hexaferrite, *AIP Advances*, 5(2015)107132.
- [12] Z. Haijun, Y. Xi, Z. Liangying, The preparation and microwave properties of  $Ba_2Zn_xCo_{2-x}Fe_{28}O_{46}$  hexaferrites, *Journal of Magnetism and Magnetic Materials*, 241(2002) 441-446.
- [13] V.N. Dhage, M.L. Mane, A.P. Keche, C.T. Birajdar, K.M. Jadhav, Structural and magnetic behaviour of aluminium doped barium hexaferrite nano particles synthesized by solution combustion technique, *Physica B:Condensed Matter* 406 (2011) 789.
- [14] M.C. Dimri, A. Verma, S.C. Kashyap, D.C. Dube, O.P. Thakur, C. Prakash, Structural, dielectric and magnetic properties of NiCuZn ferrite grown by citrate precursor method, *Journal of Material Science and Engineering B* 133 (2006) 42.
- [15] M. Hakimi, P. Alimard, M. Yousefi, Green synthesis of reduced graphene oxide/ $Sr_2CuMgFe_{28}O_{46}$  nanocomposite with tunable magnetic properties, *Ceramics International*, 40 (2014) 11957-11961.
- [16] B. X. Gu, Magnetic properties of  $Ba_2Me_2Fe_{28}O_{46}$  ( $Me_2X$ , Me=Ni, Cu, Mg, and Zn) hexaferrites, *Journal of applied physics*, 70 (1991) 372.
- [17] K.K.Mallick, P.Shepherd and R.J. Green, Dielectric properties of M-type barium hexaferrite prepared by co-precipitation, *Journal of the European Ceramic Society*, 27(2007) 2045-2052.
- [18] K.W.Wagner, The physical nature of the electrical breakdown of solid dielectrics, *Journal of the American Institute of Electrical Engineers* 41(1922)1034-1044.
- [19] R.C. Pullar, Hexagonal ferrites: A review of the synthesis, properties and applications of hexaferrite ceramics, *Progress in Materials Science*, 57(2012)1191-1334.
- [20] I. Sadiq, I. Khan, E.V. Rebrov, M.N. Ashiq, S. Naseem, M. Rana, Structural, infrared, magnetic and microwave absorption properties of rare earth doped X-type hexagonal nanoferrites, *Journal of Alloys and Compounds*, 570 (2013) 7-13.
- [21] M. A. Khan, H. Ullah, M. Junaid, M. K. Sharif, M. F. Alboud, M. F. Warsi, S. Haider, Structural, magnetic and dielectric properties of  $Yb^{3+}$  doped  $BaCo-X$  hexagonal Nanoferrites, *Journal of Alloys and Com- pounds*, S0925-8388(2016) 33852-X.
- [22] I. Ali, N. Shaheen, M. Islam, M. Irfan, M.N. Ashiq, M.A. Iqbal, A. Iftikhar, Study of electrical and dielectric behavior of  $Tb^{+3}$  substituted Y-type hexagonal ferrite, *Journal of Alloys and Compounds*, 617 (2014) 863-868.
- [23] I. Sadiq, I.Ali, E. V. Rebrov, Sh. Naseem, M.N. Ashiq, and M.U. Rana, Influence of Nd-Co Substitution on Structural, Electrical, and Dielectric Properties of X-Type Hexagonal Nanoferrites, *Journal of Materials Engineering and Performance*, 23(2014) 622-627.
- [24] M. Ahmad, I. Ali, F. Aen, M.U. Islam, M. N. Ashiq, S. Atiq, W. Ahmad, M.U. Rana, Effect of sintering temperature on magnetic and electrical properties of nano-sized  $Co_2W$  hexaferrites, *Ceramic Inter- national*, 38(2012)1267-1273.
- [25] Amrin Kagdi, Neha Solanki, Rajshree B.Jotania, Effect of sintering temperature on structural property of X-type barium-zinc Hexaferrites, *International Conference on Condensed Matter and Applied Physics*, 1728(2016)020046.
- [26] L.Z. Li, Z.Yu, Z.WenLan, K. Sun, R.DiGuo, Effects of annealing temperature on the structure and static magnetic properties of  $NiZnCo$  ferrite thin films, *Journal of Magnetism and Magnetic Materials*, 368 (2014) 8-11.
- [27] M. Ahmad, R. Grössinger, M. Kriegisch, F. Kubel, M.U. Rana, Magnetic and microwave attenuation behavior of Al-substituted  $Co_2W$  Hexaferrites synthesized by sol-gel autocombustion process, *Journal of Current Applied Physics*, 12 (2012) 1413-1420.
- [28] M.N. Ashiq, R.B. Qureshi, M.A. Malana, M.F. Ehsan, Synthesis, structural, magnetic and dielectric properties of zirconium copper doped M-type calcium strontium hexaferrites, *Journal of Alloys and Compounds*, 617 (2014) 437-443.

- [29] S. H. Mahmood, M. D. Zaqasaw, O. E. Mohsen, A. Awadallah, I. Bsoul, M. Awawdeh, Q. I. Mohaidat, Modification of the Magnetic Properties of  $\text{Co}_2\text{Y}$  Hexaferrites by Divalent and Trivalent Metal Substitutions, *Journal Solid State Phenomena*, 241(2016) 93-125.
- [30] M. Ahmad , I. Ali , F. Aen , M.U. Islam , M. N. Ashiq , S. Atiq , W. Ahmad , M.U. Rana, Effect of sintering temperature on magnetic and electrical properties of nano-sized  $\text{Co}_2\text{W}$  hexaferrites, *Journal of Ceramic Internatioal*, 38(2012) 1267-1273.
- [31] M. A. Ahmed, N.Okasha, R. M .Kershi, Could Mg content control the conduction mechanism of Ba Co Zn-W-type hexagonal ferrites?, *Journal of Magnetism and Magnetic Materials* 321 (2009) 3967–3973.
- [32] V. P.Singh , G. Kumar, P. Dhiman , R. K. Kotnala, J. Shah Khalid M. Batoor, M. Singh, Structural, dielectric and magnetic properties of nanocrystalline  $\text{BaFe}_{12}\text{O}_{19}$  hexaferrite processed via sol-gel technique, *Advanced Materials Letters*, 5(2014)447-452.
- [33] M.J. Iqbal, M.N. Asihq, P.H.Gomez, J.M.Munoz, Comparative Studies of  $\text{SrZr}_x\text{Mn}_x\text{Fe}_{12-2x}\text{O}_{19}$  Nanoparticles Synthesized by Co-precipitation and Sol-Gel Combustion Methods, *Journal of Scripta Materialia*, 47 (2007) 1093.
- [34] M.J. Iqbal , S. Farooq, Extraordinary Role of Ce-Ni Elements on the Electrical and Magnetic Properties of Sr-Ba M-Type Hexaferrites, *Journal of Materials research bulletin*, 44 (2009) 2050.